Published in final edited form as:
J Neurosci. 2013 January 30; 33(5): 1927–1939. doi:10.1523/JNEUROSCI.2080-12.2013.

THE ANTI-AGING PROTEIN KLOTHO ENHANCES OLIGODENDROCYTE MATURATION AND MYELINATION OF THE CENTRAL NERVOUS SYSTEM

Ci-Di Chen[1], **Jacob A. Sloane**[2,*], **Hu Li**[3,*], **Nurgul Aytan**[4,*], **Eustathia L. Giannaris**[5,*], **Ella Zeldich**[1], **Jason D. Hinman**[6], **Alpaslan Dedeoglu**[4], **Douglas L. Rosene**[5], **Rashmi Bansal**[7], **Jennifer Luebke**[5], **Makoto Kuro-o**[8], and **Carmela R. Abraham**[1]

[1]Department of Biochemistry, Boston University School of Medicine, Boston Massachusetts 02118

[2]Department of Neurology, Beth Israel Deaconess Medical Center, Boston Massachusetts 02215

[3]Department of Biomedical Engineering, Boston University, Boston, Massachusetts 02215

[4]Department of Neurology, Boston University School of Medicine, and Veterans Administration Boston Healthcare System, Boston Massachusetts 02130

[5]Department of Anatomy & Neurobiology, Boston University School of Medicine, Boston Massachusetts 02118

[6]Department of Neurology, University of California Los Angeles, Los Angeles California 90095

[7]Department of Neuroscience, University of Connecticut Medical School, Farmington, CT 06030

[8]University of Texas Southwestern Medical Center, Dallas Texas 75390

Abstract

We have previously shown that myelin abnormalities and loss characterize the normal aging process of the brain and that an age-associated reduction in Klotho is conserved across species. Predominantly generated in brain and kidney, Klotho overexpression extends life span, whereas loss of Klotho accelerates the development of aging-like phenotypes. While the function of Klotho in brain is unknown, loss of Klotho expression leads to cognitive deficits. In the present study, we found significant effects of Klotho on oligodendrocyte functions including induced maturation of rat primary oligodendrocytic progenitor cells (OPCs) *in vitro* and myelination. Phosphoprotein Western analysis indicated Klotho's downstream effects involve Akt and ERK signal pathways. Klotho increased OPCs maturation, and inhibition of Akt or ERK function blocked this effect on OPCs. *In vivo* studies of Klotho knockout mice and their control littermates revealed that knockout mice have a significant reduction in major myelin protein and gene expression. By immunohistochemistry, the number of total and mature oligodendrocytes was significantly lower in Klotho knockout mice. Strikingly, at the ultrastructural level, Klotho knockout mice exhibited significantly impaired myelination of the optic nerve and corpus callosum. These mice also displayed severe abnormalities at the nodes of Ranvier. In order to decipher the mechanisms by which Klotho affects oligodendrocytes, we used luciferase pathway reporters to identify the transcription factors involved. Taken together, these studies provide novel evidence for Klotho as a key player in myelin biology, which may thus be a useful therapeutic target in efforts to protect brain myelin against age-dependent changes.

Address correspondence to: Carmela R. Abraham, Department of Biochemistry, Boston University School of Medicine, 72 E. Concord Street, K304, Boston, MA 02118, Tel. 617 638-4308; Fax. 617 638-5339; cabraham@bu.edu.
*These authors contributed equally

Introduction

Klotho is an anti-aging protein named after the mythical Greek goddess who “spins the thread of life” (Kuro-o et al., 1997). Klotho knockout mice exhibit many changes that also frequently occur during human aging, including arteriosclerosis, osteoporosis, and cognitive decline. The mice develop normally but die prematurely, with an average lifespan of ~61 days (Kuro-o et al., 1997), whereas mice overexpressing Klotho live 30% longer than wild type mice (Kurosu et al., 2005). In early adulthood, Klotho knockout mice show memory retention deficits (Nagai et al., 2003b), a reduction in synapses in the hippocampus (Li et al., 2004), perturbations in axonal transport, and a neurodegenerative phenotype in the hippocampus (Shiozaki et al., 2008). Interestingly, humans carrying the Klotho-VS polymorphism exhibit reduced cognitive abilities (Deary et al., 2005; Nagai et al., 2003b), as well as reduced life span (Arking et al., 2005; Arking et al., 2003; Nagai et al., 2000). The basis of cognitive deficits in Klotho knockout mice, or in humans with Klotho-VS polymorphism is not known, and a more thorough assessment of neuropathology is needed.

Klotho is highly expressed in the choroid plexus and neurons, especially in the hippocampus, as well as in the kidney and reproductive organs (Kuro-o et al., 1997), but its function in the brain is not clear. Klotho is a type I transmembrane protein cleaved by ADAM10 and 17 from the cell membrane (Bloch et al., 2009; Chen et al., 2007), and is detectable in serum and CSF (Imura et al., 2004). Klotho functions include regulation of FGF23 signaling, suppression of the insulin/IGF1 and Wnt signaling pathways, and regulation of calcium and phosphate homeostasis (Kuro-o, 2010). In contrast to other organ systems, none of the downstream effects of Klotho have been studied for the CNS and little is known about downstream signal transduction machinery required for Klotho's CNS effects. Considering the distribution of Klotho expression and processing within the CNS and the effects on cognition cited above, Klotho is positioned to influence a variety of CNS structures and functions in development and aging.

As part of our studies of age-associated cognitive decline in the rhesus monkey, we discovered using microarray analysis that Klotho expression was decreased in the aged corpus callosum (Duce et al., 2008), likely due to the hypermethylation of its promoter (King et al., 2011). This is of interest as damage to myelin is ubiquitous in aging monkey brain (Kohama et al., 2011) at biochemical (Sloane et al., 2003), ultrastructural (Bowley et al., 2010) and macroscopic levels (Makris et al., 2007; Wisco et al., 2008) and these abnormalities are often associated with cognitive decline (Hinman and Abraham, 2007; Peters, 2009). To determine whether there is a connection between age-related alterations in Klotho expression (Duce et al., 2008) and CNS dysmyelination (Hinman and Abraham, 2007; Sloane et al., 2003), and to understand the functions of Klotho in the brain, we assessed how Klotho influences oligodendrocyte function and developmental myelination and describe here the important and novel role Klotho plays in oligodendrocyte biology and myelination.

Materials and Methods

Materials

The recombinant mouse Klotho protein containing the extracellular domain of mouse Klotho (Ala 35- Lys 982) was from R&D Systems (Minneapolis, MN). Akt inhibitor LY294002 and ERK inhibitor UO126 were from Cell Signaling (Danvers, MA). Growth factors for oligodendrocytes were from Peprotech (Rocky Hill, NJ). All other chemicals were from Sigma-Aldrich (St. Louis, MO).

Animal tissue and protein sample preparation

Klotho knockout (Kuro-o et al., 1997) and control mice were perfused with 0.1 M Phosphate buffer saline pH 7.4 at 4°C and hemibrains homogenized in 5× (v/w) ice-cold RIPA buffer with protease and phosphatase inhibitor cocktails (Roche). Samples were then centrifuged at 16,000×g for 15 min, and the supernatant was collected for SDS-PAGE and Western blot analysis.

Oligodendrocyte progenitor cell (OPC) cultures

OPCs were isolated from female Sprague-Dawley postnatal day 2 rat pups as described previously (Mi et al., 2005; Sloane and Vartanian, 2007). Cultures were maintained in high-glucose DMEM OPC culture medium (4 mM L-glutamine, 1 mM sodium pyruvate, 0.1% BSA, 50 μg/mL insulin, 30 nM sodium selenite, 10 nM D-biotin and 10 nM hydrocortisone) containing bFGF/PDGF (10 ng/mL) for 1–3 days and replaced with either DMEM medium with CNTF (10 ng/mL), T3 (15 mM) and NT3 (10 ng/mL), or DMEM with CNTF and NT3 alone, with or without recombinant mouse Klotho at a concentration of 0.4 μg/mL at 37°C for 3–8 days, as indicated in the figures. Half of the medium bathing the cells was replaced with fresh medium with or without Klotho every other day. The same concentration of Klotho was used in all experiments. The cell lysates were collected in RIPA buffer as described before, and protein samples were analyzed by SDS-PAGE and Western Blotting.

Western Blotting

Protein concentrations were measured using the Micro BCA Protein Assay Reagent Kit (Pierce, Rockford, IL) according to the manufacturer's protocol. For SDS-PAGE, cell lysates containing the same amount of total protein were boiled for 5 min and loaded on 4–20% pre-cast Tris-Glycine gels (Bio-Rad, Hercules, CA). Proteins were transferred to nitrocellulose membranes (Millipore, Billerica, MA). All antibodies were diluted in TBST (50 mM Tris, pH 8.0, 150 mM NaCl and 0.1% (v/v) Tween 20) containing 5% (w/v) nonfat dry milk. Secondary antibodies were horseradish peroxidase-conjugated goat anti-mouse, anti-rat or anti-rabbit (1:5000, Kirkegaard & Perry Laboratories, Gaithersburg, MD). Enhanced chemiluminescence (ECL) was detected using Immobilon Western Chemiluminescent Substrate (Millipore, Billerica, MA). Autoradiography was done using Kodak Scientific Imaging Film X-OMAT™ AR (Eastman Kodak, Rochester, NY).

The primary antibodies used were: anti-MBP mouse monoclonal antibody (1:1000, Covance), anti-MAG mouse monoclonal antibody (clone B11F7, 1:1000), anti-CNP mouse monoclonal antibody (1:1000, Sigma, St. Louis, MO), anti-FGF receptor substrate (FRS) Y196 (1:1000, Cell Signaling, Danvers, MA), anti-OSP rabbit polyclonal antibody (1:1000, Abcam), anti-PLP mouse monoclonal antibody (1:1000, Millipore), anti-PCNA clone PC10 (1:1000, Upstate, Temecula, CA) and anti-β-Tubulin monoclonal antibody (1:1000, Invitrogen, Carlsbad, CA). The antibodies in the Akt and ERK pathways were from phospho Akt and ERK pathway kit (Cell Signaling, Danvers, MA) and were used according to the manufacturer's protocol.

qRT-PCR

Total RNA was isolated using QIAGEN's RNeasy kit (Qiagen, Valencia, CA). A reverse transcription was performed with 2 μg of total RNA from each sample. Primers for selected mouse myelin related genes and corresponding rat oligodendrocyte maturation enriched genes as published (Cahoy et al., 2008) were designed by RealTimePrimers. Controls included beta actin (ACTB), beta-2 microglobulin (B2M), Phosphoglycerate kinase 1, hypoxanthine phosphoribosyltransferase 1 (Hprt1) and Glyceraldehyde-3-phosphate dehydrogenase (GAPDH). The qRT-PCR experiments were performed with iQ™ SYBR®

Green Supermix (Bio-rad) with detection on a Bio-rad C1000 Thermal Cycler. The whole cDNA from 2 μg of total RNA was used for one 96 well plate. Triplicates of 20 μL reactions containing primer and cDNA template were used for quantitation. A PCR reaction was carried out as follows: 1 cycle of 95°C for 3 min followed by 40 cycles of 95°C for 10 s, 55°C for 20 s, and 72°C for 30 s. This was followed by a dissociation curve beginning at 55°C and increasing by 0.2°C every 3 s, with SYBR green fluorescence measured at every interval. Relative quantitation of the difference between the control and Klotho-treated samples was done using RT^2 Profiler PCR Array Data Analysis Program from Qiagen. Genes were tested for statistical significance ($P < 0.05$), relative to the control, by student *t*-test.

Luciferase assay

Pax3 reporter plasmid (pluc-TKCD-19) was kindly provided by Dr. Frank Rauscher III (Wistar Institute, Philadelphia, PA). Signal Transduction 45 pathway Reporter Array was from SABiosciences (Qiagen, Valencia, CA). OPCs were plated into 96 well plates at a density of 0.65×10^6 cells/plate in OPC culture medium containing bFGF/PDGF for 3 days before transfection. 200 ng of Luciferase reporter or control empty-vector DNA (with 5 ng Renilla luciferase) were transfected into cells using Lipofectamine 2000 (Invitrogen), and cells were treated with or without recombinant mouse Klotho in OPC culture medium as described above. Twenty-four hours post transfection, cells were washed once with PBS and assayed for luciferase activity using the Dual-luciferase system (Promega) as described (Oh et al., 2010).

Immunofluorescence

Cells were fixed in 4% paraformaldehyde in PBS at room temperature, rinsed with PBS, and treated for 1 h with blocking solution (PBS supplemented with 0.1% Triton ×100 and 1% BSA). Cells were incubated overnight at 4°C with the primary antibody diluted in blocking solution. Cells were stained with antibodies to Olig2 (1:10,000) (Millipore), CC-1 (1:200) (Millipore), or O1 (1:2) (ATCC). Subsequently, cells were rinsed and incubated with the relevant secondary antibodies (Cy3 or Alexa-488) (Jackson ImmunoResearch) for 1 h at room temperature. Immunofluorescence images were obtained by a Nikon Eclipse 660 microscope and a SPOT-cooled CCD digital camera (Diagnostic Instruments). For every condition, we identified the maturation state of each OL for the ~30–60 cells within a given field for all fields acquired (N = 450–900 cells/condition) from 3 independent experiments. We quantified numbers of mature OLs (O1+ or CC1+) and total OL-lineage cells (Olig2+) and determined percent mature OLs of total OL-lineage cells (O1+/Olig2+ or CC1+/Olig2+) (since Olig2 labels OPCs as well as OLs).

Cell number determination, cell viability assay and LDH release

Cell number was determined colorimetrically by crystal violet staining as described previously (Zeldich et al., 2007). Cells were plated at 50,000 cells/well in 24-well plates in triplicates, and allowed to attach and spread in OPC culture medium containing bFGF/PDGF for 1–3 days and then replaced with medium containing CNTF and NT3 with or without Klotho for the indicated time periods. At the end of each time interval, the cells were washed with PBS, fixed in 70% ethanol and kept at 4°C until the staining with 1% crystal violet. Unincorporated stain was removed by washing, cells were air-dried, and the dye was extracted with 70% ethanol and optical density (absorbance 550 nm and baseline reference absorbance 750 nm) was measured by Microplate Reader (Glomax Multi Detection System, Promega, USA). The data analysis was done by subtracting the baseline readings (750 nm) from the absorbance readings (560 nm).

For cell viability assay, cells were plated in 96-well plates in six repeats, and allowed to attach and spread in OPC culture medium containing bFGF/PDGF for 3 days and then replaced with medium containing CNTF and NT3 with or without Klotho for the indicated time periods. At the end of each time interval cell number was assessed using CellTiter-Glo Luminescent Cell Viability Assay (Promega, USA) according to the manufacturer's instructions. This assay signals the presence of metabolically active cells, Briefly, 100μl of CellTiter Glo Reagent was added to the equal volume of cell culture medium present in each cell culture well. The contents were mixed for two minutes and after stabilization of the signal at RT for 10 min, the luminescence was recorded on a Microplate Reader (Glomax Multi Detection System, Promega, USA). Cell death was assessed by using the CytoTox 96 non-radioactive cytotoxicity assay (Promega, USA), which measures the LDH release into the medium.

Immunohistochemistry and cell counting in wild type and Klotho knockout mice

Five week old Klotho +/+ and −/− mice were perfused through the heart with 0.1M PBS (4°C, pH 7.4). The brains were removed and one hemisphere was immersion fixed in 4% paraformaldehyde overnight while the other was left unfixed and flash frozen with pulverized dry ice and stored at −80°C. The fixed hemisphere was removed from fixative the next day and cryoprotected in successive solutions of first 10%, then 20% glycerol in PBS with 2% DMSO (Rosene et al., 1986). The frozen hemibrains were cut in the coronal plane into 30μm thick sections with a sliding microtome. The sections were divided into six interrupted series and stored at 4°C in 0.1M PBS with 1% sodium azide as a preservative until they were processed.

For Olig2, CC-1 and GST-Pi immunohistochemistry, one series from each subject was selected and all sections were processed together in a single batch at the same time in the same reagents to eliminate any procedural variance. All steps were performed at RT unless otherwise indicated. Free-floating sections were washed, quenched with 3% hydrogen peroxide, and then blocked with 10% normal goat serum (NGS) in Phosphate Buffered Saline (PBS) with 0.4% Triton-X 100 for 1 hour. Next, sections were incubated in a stock solution (1% NGS, 0.2%Triton-X100 in 0.05M PBS) containing rabbit polyclonal anti-Olig2 antibody (Millipore ab9610, 1:10,000), mouse mAb against CC-1 (Millipore OP-80, 1:40) or anti-GST pi (Abcam, 1:500) for 48 hours at 4°C. Sections were then washed in stock solution and treated with biotinylated goat anti-rabbit or anti-mouse secondary antibody (1:600, BA5000, Vector Laboratories) for 1 hour. After washing, sections were incubated with an avidin-biotinylated horseradish peroxidase enzyme complex (PK6100, Vectastain Elite ABC kit, Vector Laboratories) for 1 hour, rinsed in KPBS, then sodium acetate buffer (0.175M), and processed with a solution of nickel sulfate hexahydrate (0.095M), 3,3 diaminobenzidine tetrahydrochloride (DAB) (0.55mM), and hydrogen peroxide (0.0025%) in 0.175M sodium acetate buffer for 15 min. The immunostained sections were mounted on gelatin-coated slides and air-dried. Then sections were defatted in chloroform:ethanol (1:1), rehydrated, counterstained with Neutral Red (1%), dehydrated in a series of ethanols, cleared in xylenes and coverslipped with Permount (Fisher Scientific).

To quantify Olig2+ and GST-Pi+ cells, the fractionator method was used to obtain a population estimate within the fimbria. The fimbria was chosen because it is an easily defined and circumscribed bundle of white matter. The fimbria was outlined in six 30 micron sections spaced 180 micron apart, starting rostrally at the level of the anterior end of the habenula and spanning approximately 1.08mm caudally using StereoInvestigator system (version 9.14.3, MBF Bioscience, Williston, VT) and a 4× Nikon Plan objective on a Nikon Eclipse E600 microscope. Cell counts were made with a 20× Nikon Plan Fluor objective. A 120 micron × 120 micron grid was overlaid on the region of interest and Olig2+ cells were counted within 40 micron × 40 micron counting frames placed at the grid intersections that

fell within the outline of the fimbria. The criterion for counting cells was the appearance of the black Ni-DAB immuno-product in the nucleus. In an adjacent series of six 30 micron thick tissue sections, GST-Pi positive cells within the fimbria were quantified. The fimbria was outlined with a 4× objective as described above. A 120 micron × 120 micron sampling grid was superimposed over the region of interest and GSTPi positive cells were counted within a 40 micron × 40 micron counting frame and 5 micron disector using a 60× Nikon Plan Fluor oil objective. A guard volume of 1 μm above the disector box was used and 2–4 micron below, depending on the thickness of the tissue section (approximately 8–10 micron total). GST-Pi positive cells had brown DAB immuno-product in the cytoplasm and nucleolus, yet the nucleus was unstained.

Nodal and paranodal immunofluorescence

Free floating 30 micron sections were stained for nodes and paranodes with rabbit anti-beta-IV spectrin (1:400) or rabbit anti-$Na_V1.6$ (1:200) (gifts from M. Rasband, Baylor College of Medicine (Ogawa et al., 2006; Rasband et al., 2003), and mouse anti-caspr (Antibodies, Inc.) (1:500), using the following protocol with all steps performed at RT unless otherwise stated. The monoclonal antibody mouse anti-caspr (clone K65/35) was developed by and obtained from the UC Davis/NIH Neuromab Facility. Sections were washed in PBS, transferred to prewarmed 10 mM sodium citrate, pH 8.5 and incubated at 80°C for 30 min for antigen retrieval. After cooling to RT, sections were washed 3 times in PBS, then blocked and permeabilized in PBS with 0.3% TX-100 (Sigma) and 10% normal donkey serum (Jackson Immunoresearch) for 30 min. Sections were then placed directly in MOM Block (Vector Labs) diluted in PBS for 1 hr, washed 3 times in PBS and then incubated overnight in primary antibody cocktails. The next day, after 3 washes in PBS, sections were incubated in donkey anti-mouse Cy2 (Jackson Immunoresearch; 1:300) and donkey anti-rabbit DyLight 549 (Jackson Immunoresearch; 1:300) for 1 hr. Sections were then mounted on gelatin subbed slides, air dried and dehydrated with 70–100% EtOH and xylene and coverslipped with DPX mounting medium.

Image acquisition was performed on a Nikon Eclipse Ti C2+ laser scanning confocal microscope. Two-micron optical sections at 100× optical objective with 2× digital zoom were obtained from five different immunolabeled sections from each of two wild-type and two Klotho-null mice. The imaged white matter included corpus callosum overlying striatum to that overlying hippocampus. Maximum intensity projections were obtained and images were postprocessed in NIS Elements software (Nikon). Nodal and paranodal segments were measured using the two-point length measurement tool. For measurement, only complete paranodal pairs (both paranodes and an immunolabeled node) were selected for measurement. A total of thirty paranodes per section (150 per animal) were measured and a total of 10 nodes per section (50 per animal) were measured. Statistical significance was determined using a Student's t-test assuming one-tail and equal variance. For presentation, images were further post-processed and cropped in Photoshop CS5 (Adobe).

Electron microscopy

35 days old Klotho +/+, +/− and −/− mice, and 25 days old Klotho −/− mice were perfused transcardially with 1% paraformaldehyde and 2.5% glutaraldehyde fixative in 0.1 M cacodylate buffer pH 7.2–7.4. Optic nerve, corpus callosum and cervical spinal cord were postfixed with 1% osmium oxide, dehydrated in alcohol series and propylene oxide before embedding in Epon. One-micrometer-thick sections were cut and stained with toluidine blue. Thin sections were contrasted with uranyl acetate and lead citrate and imaged with a JEOL (Peabody, MA) 1200EX electron microscope.

Gene set enrichment analysis (GSEA)

GSEA was performed according to Subramanian et al. (Subramanian et al., 2005) with 1186 chemical and genetic perturbation (CGP) gene sets. Klotho −/− mice versus Wild-type +/+ mice gene expression profiles were ranked based on P value. The ranked gene list was utilized as input for the CGP gene sets. The significant gene sets were selected based on the normalized enrichment score (NES) and false discovery rate (FDR), accordingly.

Results

Klotho effects on primary oligodendrocytes in vitro

Klotho has been reported to affect intracellular signaling through Akt and ERK1/2 pathways in HEK293 and breast cancer cells (Kurosu et al., 2006; Wolf et al., 2008). We therefore assessed whether Klotho induces ERK1/2 and Akt protein phosphorylation from 0 to 60 min in OPCs isolated from rat brain. Western blot results indicated that proteins in the ERK1/2 and Akt pathway including PTEN (Ser380), Akt (Ser473), and GSK-3β (Ser9) were phosphorylated upon Klotho treatment (Figure 1). We found two waves of GSK3βphosphorylation in OPCs upon Klotho treatment, with a first peak at 10 min and a second at 45 min (Figure 1). These results suggest that the Akt and ERK/12 pathways are both involved in Klotho-induced signaling in rat primary OPCs. We also examined phosphorylation of FGF receptor substrate 2 (FRS2) since Klotho may function by modulating FGF signal transduction pathways (Kurosu et al., 2006; Urakawa et al., 2006). Western blot results indicated that FRS2 was phosphorylated at Y196 upon Klotho treatment (Figure 1), suggesting that the FGF signaling pathways may be involved in Klotho-induced signaling in rat OPCs. However, it is also possible that Klotho affects FRS2 phosphorylation via Klotho's interaction with the TrkA receptor (Meakin et al., 1999).

To examine the effects of Klotho on the OPC phenotype, oligodendrocyte maturation was assessed by immunohistochemistry for mature oligodendrocytes (O1), and pan-oligodendrocytes (Olig2) after Klotho treatment. The OPCs were allowed to attach and spread in OPC culture medium containing bFGF/PDGF for 3 days and then replaced with medium containing CNTF and NT3 with or without Klotho. Following 3 and 6 day Klotho treatment, we found that Klotho increased the percentage of mature primary oligodendrocytes (% O1/Olig2) (Figure 2A and B). Similar results were obtained using another marker of mature oligodendrocytes, CC-1, (Figure 2C). Klotho enhances OPC maturation in medium containing CNTF and T3, or in medium containing CNTF, T3 and NT3 (Figure 2D). Since both Akt and ERK1/2 phosphorylation occurred rapidly after exposure to Klotho, we asked whether Akt and ERK1/2 function is required for Klotho's effects on OPC maturation. OPCs were treated with Klotho in the presence or absence of Akt and ERK inhibitors (LY294002 (LY) for Akt inhibition or UO126 (UO) for ERK inhibition). Inhibition of ERK function reduced, while Akt functional inhibition completely abolished the effects of Klotho on OPC maturation (Figure 2E), suggesting that Klotho enhances OPC maturation primarily via signaling requiring Akt but also, to a more limited degree, through ERK1/2. Western blot analysis of Klotho-treated OPCs revealed that Klotho enhanced the expression of the major myelin proteins including myelin-associated glycoprotein (MAG), myelin basic protein (MBP), oligodendrocyte specific protein (OSP/Claudin11), and proteolipid protein (PLP) (Figure 2F and G), confirming that Klotho enhances OPC maturation *in vitro*. Western blotting for the cell proliferation marker, PCNA, revealed no difference with Klotho treatment (Figure 4F and G), suggesting Klotho does not enhance OPC proliferation. We also examined cell number and cell viability by crystal violet staining and CellTiterGlo assay which reflects the amount of the ATP present, and we found no difference in Klotho treated and untreated OPCs from day 1 to day 4 in the cell viability assay and for day 2 and day 4 for crystal violet staining (Figure 2H and I). Since

OPCs were allowed to attach and spread for 3 days in the presence of basic FGF (bFGF) and PDGF, cell proliferation occurred during this period. After we treated the OPCs with Klotho in culture medium containing CNTF and T3, OPCs started to differentiate but cell numbers remained constant as shown in Figure 2H and I. We also observed no difference with a cell death assay by measuring LDH release to the media with or without Klotho. These results suggest that Klotho affects oligodendrocyte differentiation and maturation, but not their proliferation and cell death.

qRT-PCR analysis of Klotho effect on OPC maturation

Recently a transcriptome database for astrocytes, neurons and oligodendrocytes has been published providing cell type specific markers for these neural cells (Cahoy et al., 2008). To confirm the effect of Klotho on OPC maturation, we performed qRT-PCR analysis of the top 45 genes (see Table 4 for primers information) from the OL maturation enriched gene list (Cahoy et al., 2008) using RNA isolated from OPCs treated with Klotho or PBS only, for 3 or 7 days. qRT-PCR revealed that comparing 3 days and 7 days differentiated OPC, most of the genes were highly expressed at day 7 but had either low or undetectable expression at day 3 (Figure 3A), suggesting the primer sets were working well to detect OPC maturation enriched genes. We then analyzed the gene expression changes of RNA from OPC treated with Klotho for 7 days compared to PBS-treated control. We found that 37 out of the 45 genes were detectable, and 78% (29/37) of the genes were up-regulated by Klotho. Of those 37, 21 genes reached significance of $p<0.05$ (Figure 3B). The qPCR results were consistent with the results obtained from protein expression as assessed by WB in that the expression of major myelin proteins was enhanced 2–3 folds in response to exogenous addition of Klotho (Figure 2F and G). These results demonstrate that Klotho can enhance OPC maturation as shown by the immunostaining of the cells with two separate oligodendrocyte markers O1 and CC-1, and by WB analyses as shown in Figures 2B, D, F and G.

Effects of Klotho absence in vivo in Klotho knockout mice

If Klotho is important for oligodendrocyte maturation *in vitro*, Klotho knockout mice should exhibit deficiencies in myelination. The ultrastructure of 35-day-old Klotho knockout (−/−), hemizygous (+/−) and control (−/−) mice brains was examined by electron microscopy. There was a significant reduction in the percentage of myelinated fibers in both optic nerve and corpus callosum, but not cervical spinal cord (Figure 4), suggestive of region-specific effects of Klotho expression. In the optic nerve, Klotho −/− mice exhibited a drastic reduction in the percentage of myelinated fibers (10% compared to 90% in +/+ littermates) (Figure 4E, F and M), while Klotho +/− mice showed normal numbers of myelinated fibers (Figure 5C and D compared to A and B). In the corpus callosum, both Klotho +/− and Klotho −/− exhibited significantly impaired myelination (20% compared to 90% in +/+ mice) (Figure 4G–M). No significant change was seen in the percentage of myelinated fibers in the spinal cord (Figure 4M). A similar reduction in the myelination of fibers in the corpus callosum was found in two 25 day-old Klotho knockout brains, with only 16.4±1.6% fibers being myelinated.

In order to decipher the potential basis for region-specific effects of Klotho, we examined the distribution of Klotho in the corpus callosum, spinal cord and optic nerve from five 1.1 and five 1.6 month-old mice. The results showed that Klotho was expressed in all three regions, with the highest expression in the corpus callosum, and lowest in spinal cord at the younger age (1.1 months, Figure 4N and O). The results of the WBs of the three specific brain samples represent the levels of available Klotho protein surrounding these three brain regions. A higher Klotho level, e.g, corpus callosum, implies that Klotho's function is needed in that region, and less Klotho suggests Klotho is less necessary, e.g, spinal cord. These data, together with the EM results, suggest that Klotho is required for proper

myelination of fibers in the corpus callosum. We therefore examined the myelin markers myelin associated glycoprotein (MAG), MBP, and 2', 3'cyclic nucleotide-3'-phosphodiesterase (CNP) in brain tissues of 8 week old Klotho knockout and control mice. Western blot analyses demonstrated significant reduction of major myelin proteins in Klotho deficient mice compared to control mice (Figure 4P and Q) indicating that Klotho affects myelination via inducing myelin protein production by oligodendrocytes.

To assess the effects of the hypomyelination seen in Klotho −/− mice on axonal microdomain organization, free-floating sections were stained for caspr to label paranodes, and beta-IV spectrin or $Na_v1.6$ to label nodes. No differences were seen in nodal staining patterns between beta-IV spectrin and $Na_v1.6$ immunolabels. High magnification confocal optical sections reveal that within the corpus callosum, Klotho −/− mice show a significant decrease in paranodal length compared to wild-type controls (Figure 5). This decrease in paranodal length suggests that there is less robust myelination in each axon in the Klotho −/− mice consistent with hypomyelination seen in the ultrastructural analysis. While the absolute difference in paranodal length is small (0.30 microns), this average value would translate to one less paranodal loop per axon (assuming each loop is roughly 0.25 microns, (Trapp and Kidd, 2004)). The decrease in paranodal length was associated with a corresponding significant increase in nodal length by 0.25 microns (Figure 5E). Analysis of nodal and paranodal domains in the corpus callosum (Figure 5F) and optic nerve (data not shown) by electron microscopy did not demonstrate any ultrastructural changes in axonal microdomains. Since nodal length shortens during myelination (Dugandzija-Novakovic et al., 1995; Vabnick et al., 1996), this increase in nodal length likely represents more immature nodal segments in Klotho −/− mice. Longer nodes may be more energetically unstable and lead to progressive axonal degeneration (Waxman, 1998).

Immunohistochemistry and quantitative analysis of brain sections from Klotho knockout mice at 5 weeks of age showed a ~30% reduction in the numbers of Olig2+ oligodendrocyte-lineage cells in the fimbria compared to control mice (Figure 6A–E). In the corpus callosum, we detected a similar trend towards a significant reduction in Olig2+ cells in Klotho knockout mice (data not shown). In addition, we found a similar and confirmatory reduction (21%) in the number of mature oligodendrocytes immuno-positive for the GST-Pi marker (Mason et al., 2004), suggestive of reduced levels of GST-Pi-positive mature oligodendrocytes in the fimbria of Klotho null mice compared to control mice (Figure 6F–J).

In order to determine whether these changes in the expression of myelin proteins are also seen at the mRNA level, we performed microarray analysis using RNA from 8 weeks old Klotho +/+ and −/− mice brain tissue, and applied gene set enrichment analysis to identify which canonical pathways were involved. With this approach, we found that a set of myelin related genes were downregulated. To examine whether Klotho affects gene expression of these myelin related genes, we performed qRT-PCR analysis of the 15 myelin-related genes. The qRT-PCR results revealed that all of the myelin related genes tested were reduced compared to control mice, and 11 out of 15 genes were down-regulated more than 2 fold (Table 1). The results demonstrate that lack of Klotho resulted in reduction in expression of major myelin genes.

To identify potential transcription factors involved in Klotho-mediated responses in OPCs, we examined regulatory effects of Klotho using a signaling pathway luciferase reporter system. We optimized transfection efficiency in primary oligodendrocytic cells by testing 15 available transfection reagents and found that Lipofectamine 2000 (Invitrogen) was superior for the luciferase reporter system in these cells (data not shown). We then tested 45 signaling pathway reporters (Qiagen, see Table 2) in OPCs with or without Klotho treatment. In addition, we also tested the Pax3 reporter since Pax3 repression is directly

relevant to oligodendrocyte maturation to a myelinating phenotype (He et al., 2007). The results showed that Klotho inhibited C/EBP, AP1, NFkB, and Pax3 activities, while it enhanced LXR, ARE, STAT3, PR, and SRE MAPK/ERK transcription factor activities (Figure 7B, Table 3). The effect of Klotho on STAT3 phosphorylation in OPCs was also confirmed by Western blot (Figure 7A). These results revealed the possible transcription factors involvement in Klotho-mediated responses in OPCs.

Discussion

Klotho affects oligodendrocyte maturation and myelination

In prior work, our group discovered reductions in Klotho in the aging brain white matter (Duce et al., 2008), where myelin deficits are also observed (Hinman and Abraham, 2007), suggesting a connection between Klotho expression and myelination. Thus, in this manuscript, we focused on the effect of Klotho on oligodendrocytes, the myelinating cells of the CNS. Our findings indicate a dramatic and important effect of Klotho on oligodendrocyte maturation and on myelination. Klotho enhances expression of MBP, MAG, PLP and OSP/claudin11, all being major myelin proteins, and induces OPC maturation *in vitro. In vivo*, Klotho knockout mice suffer from severe hypomyelination of the optic nerve and corpus callosum, which alters axonal microdomain organization. Myelin defects associated with loss of Klotho expression strongly indicate that decreased Klotho expression could result in slowed action potential propagation, conduction block, and destabilized coordinated neuronal communication, as seen in hypomyelinating and demyelinating diseases (Hanafy and Sloane, 2011; Hinman and Abraham, 2007). The numbers of myelinated fibers in the optic nerves and corpus callosum of the Klotho knockout mice were much lower that in the wild type mice, as determined by EM studies (Figure 4). However, the numbers of mature and total oligodendrocytes in the fimbria were reduced by a lower percentage (Figure 6). These data suggest that those oligodendrocytes that appear mature as judged by their staining with GST-Pi, were not able to myelinate axons properly, indicating an important role of Klotho in the myelination process.

Klotho-activated signaling pathways include Akt and ERK1/2

We found that Akt and ERK1/2 signaling likely regulate OPC cells subjected to Klotho treatment. This finding is consistent with the data reported by Wolf et al. who found that both pathways were involved in Klotho-treated HEK293 and breast cancer cells (Wolf et al., 2008). Moreover, a recent study reported that Klotho induced ERK/MEK phosphorylation in HUVEC cells (Maekawa et al., 2011). Our results also suggest that Klotho could act on an as-yet unidentified Klotho receptor expressed on oligodendrocytes.

Oligodendrocyte development is regulated by numerous growth factors, which can signal through Akt and ERK1/2 dependent pathways (Bansal et al., 2003; Baron et al., 2000; Bhat and Zhang, 1996; Bibollet-Bahena et al., 2009; Cui and Almazan, 2007; Du et al., 2006; Fortin et al., 2005; Frederick et al., 2007; Frost et al., 2009; Fyffe-Maricich et al., 2011; Guardiola-Diaz et al., 2012; Van't Veer et al., 2009; Younes-Rapozo et al., 2009). Klotho has been reported to regulate insulin/IGF-1, FGF23, and Wnt signaling (Kuro-o, 2006, 2008a). In OPCs, Klotho is unlikely to function through IGF-1 signaling since Klotho inhibits the insulin/IGF-1 signaling pathway (Kurosu et al., 2005) and IGF-1 was reported to enhance OPC maturation and myelination (Bibollet-Bahena and Almazan, 2009). It is unknown whether FGF23 for which Klotho serves as a co-receptor in the kidney, has a role in neurodevelopment. However, our findings show that Klotho treatment of OPCs induces the phosphorylation of FRS2, a positive regulator of FGF signaling upstream of Akt and Erk pathway which is phosphorylated in oligodendrocytes upon activation of FGF-receptor (Bryant et al., 2009). Another putative receptor on OPCs is the NGF receptor, TrkA, since

FRS2 is able to bind directly to both FGF and NGF receptors (Meakin et al., 1999; Ong et al., 2000). Possibly, Klotho functions through the FGF signaling pathway indirectly via another FGF ligand, or Klotho could modulate signaling of other cytokines in astrocytes via FGF signaling, as has been shown for insulin/IGF-1 signaling in C. elegans (Chateau et al., 2010). We cannot rule out the possibility that Klotho sequesters a ligand and blocks its accessibility to the receptor, or that Klotho binds directly to a receptor to prevent a ligand-receptor interaction. Another reported mechanism for Klotho effects is via the inhibition of the Wnt/β-catenin pathway, where Klotho may function as a secreted Wnt antagonist (Liu et al., 2007). Activating the Wnt/β-catenin pathway delays the development of myelinating oligodendrocytes (Fancy et al., 2009; Feigenson et al., 2009), while Olig2-induced neuronal stem cell differentiation into mature oligodendrocytes involves downregulation of the Wnt signaling pathway (Ahn et al., 2008). Whether Klotho stimulates oligodendrocyte maturation through the Wnt or insulin/IGF signaling pathways in addition to the FGF and NGF pathways is currently under investigation. It is interesting to note that *in vivo*, FGFR1/2 and ERK1/2 MAPK signaling in oligodendrocytes has recently been shown to regulate the growth of the myelin sheath, independent of oligodendrocyte differentiation (Furusho et al., 2012; Ishii et al., 2012).

Potential transcription factors involved in Klotho-mediated responses

We identified a set of transcription factors (TF) potentially involved in Klotho-dependent effects on OPC cells using the luciferase reporter system. Several of the TFs have been reported previously to be associated with Klotho functions, including C/EBP, AP1/JNK, NFkB, STAT3, and SRE MAPK/ERK (Chihara et al., 2006; Hsieh et al., 2010; Liu et al., 2011; Medici et al., 2008; Thurston et al., 2010; Wolf et al., 2008; Yamamoto et al., 2005; Zhao et al., 2011). Klotho protein increases resistance to oxidative stress at the cellular and organismal level in mammals (Kurosu et al., 2005; Nagai et al., 2003b; Rakugi et al., 2007; Shih and Yen, 2007). Klotho-deficient mice have impaired cognitive function when compared with wild-type mice, and treatment with the antioxidant α-tocopherol improves cognition (Nagai et al., 2003a), suggesting that Klotho may function as a neuroprotective factor. In addition, Klotho protein showed a neuroprotective effect on human neural stem cells (Foster et al., 2011), likely through the anti-oxidative stress effect of Klotho. We found an increase in the antioxidant response element (ARE) activity, which indicates that the antioxidative function of Klotho may be involved in the protection of oligodendrocytes. The new TF activities identified to be associated with Klotho include Pax3, LXR, and the progesterone receptor (PR). LXRs are oxysterol and nuclear receptors, which play an important role in the control of cholesterol homeostasis (Repa and Mangelsdorf, 2000; Whitney et al., 2002).

Implications of Klotho induced transcription factor changes for oligodendrocyte biology

The lack of LXRs in mice leads to disorganized myelin sheaths, suggesting a role for the LXRs in myelination (Wang et al., 2002). Paired homeodomain protein 3 (Pax3) is important for development of myelinating glia and the myelination process (Wegner, 2000). An inverse correlation was observed between expression of Pax3 and MBP, suggesting that it represses MBP transcription (Kioussi et al., 1995). We found that Klotho inhibited Pax3 reporter activity and increased MBP expression in OPCs, therefore, we speculate that Klotho may increase MBP through the Pax3 pathway. Further investigation is required to decipher the direct or indirect involvement of the Pax3 transcription factor pathway resulting in Klotho's effects on oligodendrocytes. The transcription factor STAT3 has been previously reported to be involved in oligodendrocyte differentiation (Dell'Albani et al., 1998; Massa et al., 2000). Klotho treatment induced STAT3 phosphorylation, which is required for STAT3 activity (Bromberg and Darnell, 2000). Furthermore, the protein tyrosine phosphatase SHP-1 regulates oligodendrocyte differentiation through STAT3 in response to the IL-6

family of cytokines (Massa et al., 2000). Thus, Klotho may also act through STAT3 to drive OPC maturation.

Regardless of which receptor, signaling pathway(s), and transcription factors are involved, our *in vitro* and *in vivo* studies indicate that Klotho clearly has a significant regulatory role in OPC maturation and developmental myelination. Interestingly, Klotho has been reported to have a role in cell differentiation of diverse systems throughout the body including bone, fat and the cardiovascular system (Chihara et al., 2006; Kawaguchi et al., 1999; Shimada et al., 2004). Klotho gene expression appears to cause the impairment of both osteoblast and osteoclast differentiation (Kawaguchi et al., 1999). In addition, both angiogenesis and vasculogenesis are impaired in Klotho mutant mice, suggesting a role for Klotho in differentiation of endothelial precursor cells (Shimada et al., 2004). As a humoral factor, Klotho works to promote expression of differentiation markers in 3T3-L1 cells, indicating Klotho may play an essential role in adipocyte differentiation (Chihara et al., 2006).

In summary, we demonstrate a novel function of Klotho in oligodendrocyte maturation and developmental myelination of the CNS. This role is in addition to Klotho's function as a neuroprotective factor through preventing neurons from oxidative damage as proposed (Kuro-o, 2008b). Klotho may function as a humoral factor secreted by neurons or choroid plexus to promote myelination in neurodevelopment. It is possible that Klotho plays a regulatory role in maintaining or supporting oligodendrocyte and OPC function in the adult CNS, once the development has plateaued. Since we observed downregulation of Klotho in aged brain white matter, it is plausible that reduced Klotho level may account for damage to myelin and age-associated cognitive decline, and increasing Klotho level may protect myelin integrity and prevent myelin degeneration in the aged brain. Klotho is thus a new member of the large family of proteins that are crucial to neuron-oligodendrocyte communication, and studies on the functions of Klotho are likely to provide new therapeutic approaches for diseases in which myelin abnormalities play important pathogenic roles such as multiple sclerosis and schizophrenia (Edgar et al., 2004; Taveggia et al.).

Acknowledgments

We are grateful to Dr. Alan Peters for help in interpretation of the EM data. We thank Drs. Yuriy Alekseyev and Marc Lenburg for help with the microarray analysis and Drs. Sha Mi, Paul Rosenberg and Ms. Jianlin Wang for help with the early rat OPC preparations. We thank Dr. Cindy Lemere and Mr. Jeffrey Frost for the mice samples and help in isolating mouse brain tissues, Dr. Rong Fan for help in preparing Klotho mice brain tissue homogenates, and Ms. Chun-Tsin Hsu for assistance with the qRT-PCR experiments. We thank Dr. Matt Rasband for sharing of antibody reagents. We thank Drs. Gwendalyn King, James J. Collins, Ji-Hye Paik, Ido Wolf and Tami Rubinek for critical review of and suggestions for the manuscript, This work was supported by NIH-NIA grant AG-00001, an ADDF award to CRA, a NIH-NINDS R25 Training Grant to JDH, a National Multiple Sclerosis Society Research Grant to JAS, and an Ellison Foundation Award to CC.

Abbreviations

PCR	polymerase chain reaction
DMEM	Dulbecco's modified Eagle's Medium
PBS	phosphate buffered saline
FBS	fetal bovine serum
BSA	bovine serum albumin
SDS-PAGE	sodium dodecyl sulfate polyacrylamide gel electrophoresis
MAG	myelin associated glycoprotein

MBP	myelin basic protein
CNP	2', 3'cyclic nucleotide-3'-phosphodiesterase
OPCs	oligodendrocyte precursor cells
SI	supporting information.

References

Ahn SM, Byun K, Kim D, Lee K, Yoo JS, Kim SU, Jho EH, Simpson RJ, Lee B. Olig2-induced neural stem cell differentiation involves downregulation of Wnt signaling and induction of Dickkopf-1 expression. PLoS One. 2008; 3:e3917. [PubMed: 19093005]

Arking DE, Atzmon G, Arking A, Barzilai N, Dietz HC. Association between a functional variant of the KLOTHO gene and high-density lipoprotein cholesterol, blood pressure, stroke, and longevity. Circ Res. 2005; 96:412–418. [PubMed: 15677572]

Arking DE, Becker DM, Yanek LR, Fallin D, Judge DP, Moy TF, Becker LC, Dietz HC. KLOTHO allele status and the risk of early-onset occult coronary artery disease. Am J Hum Genet. 2003; 72:1154–1161. [PubMed: 12669274]

Bansal R, Magge S, Winkler S. Specific inhibitor of FGF receptor signaling: FGF-2-mediated effects on proliferation, differentiation, and MAPK activation are inhibited by PD173074 in oligodendrocyte-lineage cells. Journal of neuroscience research. 2003; 74:486–493. [PubMed: 14598292]

Baron W, Metz B, Bansal R, Hoekstra D, de Vries H. PDGF and FGF-2 signaling in oligodendrocyte progenitor cells: regulation of proliferation and differentiation by multiple intracellular signaling pathways. Mol Cell Neurosci. 2000; 15:314–329. [PubMed: 10736207]

Bhat NR, Zhang P. Activation of mitogen-activated protein kinases in oligodendrocytes. Journal of neurochemistry. 1996; 66:1986–1994. [PubMed: 8780027]

Bibollet-Bahena O, Almazan G. IGF-1-stimulated protein synthesis in oligodendrocyte progenitors requires PI3K/mTOR/Akt and MEK/ERK pathways. Journal of neurochemistry. 2009; 109:1440–1451. [PubMed: 19453943]

Bibollet-Bahena O, Cui QL, Almazan G. The insulin-like growth factor-1 axis and its potential as a therapeutic target in central nervous system (CNS) disorders. Cent Nerv Syst Agents Med Chem. 2009; 9:95–109. [PubMed: 20021343]

Bloch L, Sineshchekova O, Reichenbach D, Reiss K, Saftig P, Kuro-o M, Kaether C. Klotho is a substrate for alpha-, beta- and gamma-secretase. FEBS Lett. 2009; 583:3221–3224. [PubMed: 19737556]

Bowley MP, Cabral H, Rosene DL, Peters A. Age changes in myelinated nerve fibers of the cingulate bundle and corpus callosum in the rhesus monkey. The Journal of comparative neurology. 2010; 518:3046–3064. [PubMed: 20533359]

Bromberg J, Darnell JE Jr. The role of STATs in transcriptional control and their impact on cellular function. Oncogene. 2000; 19:2468–2473. [PubMed: 10851045]

Bryant MR, Marta CB, Kim FS, Bansal R. Phosphorylation and lipid raft association of fibroblast growth factor receptor-2 in oligodendrocytes. Glia. 2009; 57:935–946. [PubMed: 19053057]

Cahoy JD, Emery B, Kaushal A, Foo LC, Zamanian JL, Christopherson KS, Xing Y, Lubischer JL, Krieg PA, Krupenko SA, et al. A transcriptome database for astrocytes, neurons, and oligodendrocytes: a new resource for understanding brain development and function. The Journal of neuroscience : the official journal of the Society for Neuroscience. 2008; 28:264–278. [PubMed: 18171944]

Chateau MT, Araiz C, Descamps S, Galas S. Klotho interferes with a novel FGF-signalling pathway and insulin/Igf-like signalling to improve longevity and stress resistance in Caenorhabditis elegans. Aging (Albany NY). 2010; 2:567–581. [PubMed: 20844315]

Chen CD, Podvin S, Gillespie E, Leeman SE, Abraham CR. Insulin stimulates the cleavage and release of the extracellular domain of Klotho by ADAM10 and ADAM17. Proc Natl Acad Sci U S A. 2007; 104:19796–19801. [PubMed: 18056631]

Chihara Y, Rakugi H, Ishikawa K, Ikushima M, Maekawa Y, Ohta J, Kida I, Ogihara T. Klotho protein promotes adipocyte differentiation. Endocrinology. 2006; 147:3835–3842. [PubMed: 16709611]

Cui QL, Almazan G. IGF-I-induced oligodendrocyte progenitor proliferation requires PI3K/Akt, MEK/ERK, and Src-like tyrosine kinases. Journal of neurochemistry. 2007; 100:1480–1493. [PubMed: 17348861]

Deary IJ, Harris SE, Fox HC, Hayward C, Wright AF, Starr JM, Whalley LJ. KLOTHO genotype and cognitive ability in childhood and old age in the same individuals. Neuroscience letters. 2005; 378:22–27. [PubMed: 15763166]

Dell'Albani P, Kahn MA, Cole R, Condorelli DF, Giuffrida-Stella AM, de Vellis J. Oligodendroglial survival factors, PDGF-AA and CNTF, activate similar JAK/STAT signaling pathways. Journal of neuroscience research. 1998; 54:191–205. [PubMed: 9788278]

Du Y, Lercher LD, Zhou R, Dreyfus CF. Mitogen-activated protein kinase pathway mediates effects of brain-derived neurotrophic factor on differentiation of basal forebrain oligodendrocytes. Journal of neuroscience research. 2006; 84:1692–1702. [PubMed: 17044032]

Duce JA, Podvin S, Hollander W, Kipling D, Rosene DL, Abraham CR. Gene profile analysis implicates Klotho as an important contributor to aging changes in brain white matter of the rhesus monkey. Glia. 2008; 56:106–117. [PubMed: 17963266]

Dugandzija-Novakovic S, Koszowski AG, Levinson SR, Shrager P. Clustering of Na+ channels and node of Ranvier formation in remyelinating axons. The Journal of neuroscience : the official journal of the Society for Neuroscience. 1995; 15:492–503. [PubMed: 7823157]

Edgar JM, McLaughlin M, Barrie JA, McCulloch MC, Garbern J, Griffiths IR. Age-related axonal and myelin changes in the rumpshaker mutation of the Plp gene. Acta neuropathologica. 2004; 107:331–335. [PubMed: 14745569]

Fancy SP, Baranzini SE, Zhao C, Yuk DI, Irvine KA, Kaing S, Sanai N, Franklin RJ, Rowitch DH. Dysregulation of the Wnt pathway inhibits timely myelination and remyelination in the mammalian CNS. Genes & development. 2009; 23:1571–1585. [PubMed: 19515974]

Feigenson K, Reid M, See J, Crenshaw EB 3rd, Grinspan JB. Wnt signaling is sufficient to perturb oligodendrocyte maturation. Molecular and cellular neurosciences. 2009; 42:255–265. [PubMed: 19619658]

Fortin D, Rom E, Sun H, Yayon A, Bansal R. Distinct fibroblast growth factor (FGF)/FGF receptor signaling pairs initiate diverse cellular responses in the oligodendrocyte lineage. The Journal of neuroscience : the official journal of the Society for Neuroscience. 2005; 25:7470–7479. [PubMed: 16093398]

Foster PP, Rosenblatt KP, Kuljis RO. Exercise-induced cognitive plasticity, implications for mild cognitive impairment and Alzheimer's disease. Front Neurol. 2011; 2:28. [PubMed: 21602910]

Frederick TJ, Min J, Altieri SC, Mitchell NE, Wood TL. Synergistic induction of cyclin D1 in oligodendrocyte progenitor cells by IGF-I and FGF-2 requires differential stimulation of multiple signaling pathways. Glia. 2007; 55:1011–1022. [PubMed: 17508424]

Frost EE, Zhou Z, Krasnesky K, Armstrong RC. Initiation of oligodendrocyte progenitor cell migration by a PDGF-A activated extracellular regulated kinase (ERK) signaling pathway. Neurochemical research. 2009; 34:169–181. [PubMed: 18512152]

Furusho M, Dupree JL, Nave KA, Bansal R. Fibroblast growth factor receptor signaling in oligodendrocytes regulates myelin sheath thickness. The Journal of neuroscience : the official journal of the Society for Neuroscience. 2012; 32:6631–6641. [PubMed: 22573685]

Fyffe-Maricich SL, Karlo JC, Landreth GE, Miller RH. The ERK2 mitogen-activated protein kinase regulates the timing of oligodendrocyte differentiation. The Journal of neuroscience : the official journal of the Society for Neuroscience. 2011; 31:843–850. [PubMed: 21248107]

Guardiola-Diaz HM, Ishii A, Bansal R. Erk1/2 MAPK and mTOR signaling sequentially regulates progression through distinct stages of oligodendrocyte differentiation. Glia. 2012; 60:476–486. [PubMed: 22144101]

Hanafy KA, Sloane JA. Regulation of remyelination in multiple sclerosis. FEBS letters. 2011; 585:3821–3828. [PubMed: 21443876]

He Y, Dupree J, Wang J, Sandoval J, Li J, Liu H, Shi Y, Nave K, Casaccia-Bonnefil P. The transcription factor Yin Yang 1 is essential for oligodendrocyte progenitor differentiation. Neuron. 2007; 55:217–230. [PubMed: 17640524]

Hinman JD, Abraham CR. What's behind the decline? The role of white matter in brain aging. Neurochem Res. 2007; 32:2023–2031. [PubMed: 17447140]

Hsieh CC, Kuro-o M, Rosenblatt KP, Brobey R, Papaconstantinou J. The ASK1-Signalosome regulates p38 MAPK activity in response to levels of endogenous oxidative stress in the Klotho mouse models of aging. Aging (Albany NY). 2010; 2:597–611. [PubMed: 20844314]

Imura A, Iwano A, Tohyama O, Tsuji Y, Nozaki K, Hashimoto N, Fujimori T, Nabeshima Y. Secreted Klotho protein in sera and CSF: implication for post-translational cleavage in release of Klotho protein from cell membrane. FEBS Lett. 2004; 565:143–147. [PubMed: 15135068]

Ishii A, Fyffe-Maricich SL, Furusho M, Miller RH, Bansal R. ERK1/ERK2 MAPK Signaling is Required to Increase Myelin Thickness Independent of Oligodendrocyte Differentiation and Initiation of Myelination. The Journal of neuroscience : the official journal of the Society for Neuroscience. 2012; 32:8855–8864. [PubMed: 22745486]

Kawaguchi H, Manabe N, Miyaura C, Chikuda H, Nakamura K, Kuro-o M. Independent impairment of osteoblast and osteoclast differentiation in klotho mouse exhibiting low-turnover osteopenia. J Clin Invest. 1999; 104:229–237. [PubMed: 10430604]

King GD, Rosene DL, Abraham CR. Promoter methylation and age-related downregulation of Klotho in rhesus monkey. Age (Dordr). 2011

Kioussi C, Gross MK, Gruss P. Pax3: a paired domain gene as a regulator in PNS myelination. Neuron. 1995; 15:553–562. [PubMed: 7546735]

Kohama SG, Rosene DL, Sherman LS. Age-related changes in human and non-human primate white matter: from myelination disturbances to cognitive decline. Age (Dordr). 2011

Kuro-o M. Klotho. Pflugers Arch. 459:333–343. [PubMed: 19730882]

Kuro-o M. Klotho as a regulator of fibroblast growth factor signaling and phosphate/calcium metabolism. Curr Opin Nephrol Hypertens. 2006; 15:437–441. [PubMed: 16775459]

Kuro-o M. Endocrine FGFs and Klothos: emerging concepts. Trends Endocrinol Metab. 2008a; 19:239–245. [PubMed: 18692401]

Kuro-o M. Klotho as a regulator of oxidative stress and senescence. Biol Chem. 2008b; 389:233–241. [PubMed: 18177265]

Kuro-o M. Klotho. Pflugers Archiv : European journal of physiology. 2010; 459:333–343. [PubMed: 19730882]

Kuro-o M, Matsumura Y, Aizawa H, Kawaguchi H, Suga T, Utsugi T, Ohyama Y, Kurabayashi M, Kaname T, Kume E, et al. Mutation of the mouse klotho gene leads to a syndrome resembling ageing. Nature. 1997; 390:45–51. [PubMed: 9363890]

Kurosu H, Ogawa Y, Miyoshi M, Yamamoto M, Nandi A, Rosenblatt KP, Baum MG, Schiavi S, Hu MC, Moe OW, et al. Regulation of fibroblast growth factor-23 signaling by klotho. J Biol Chem. 2006; 281:6120–6123. [PubMed: 16436388]

Kurosu H, Yamamoto M, Clark JD, Pastor JV, Nandi A, Gurnani P, McGuinness OP, Chikuda H, Yamaguchi M, Kawaguchi H, et al. Suppression of aging in mice by the hormone Klotho. Science. 2005; 309:1829–1833. [PubMed: 16123266]

Li SA, Watanabe M, Yamada H, Nagai A, Kinuta M, Takei K. Immunohistochemical localization of Klotho protein in brain, kidney, and reproductive organs of mice. Cell Struct Funct. 2004; 29:91–99. [PubMed: 15665504]

Liu F, Wu S, Ren H, Gu J. Klotho suppresses RIG-I-mediated senescence-associated inflammation. Nature cell biology. 2011; 13:254–262.

Liu H, Fergusson MM, Castilho RM, Liu J, Cao L, Chen J, Malide D, Rovira II, Schimel D, Kuo CJ, et al. Augmented Wnt signaling in a mammalian model of accelerated aging. Science. 2007; 317:803–806. [PubMed: 17690294]

Maekawa Y, Ohishi M, Ikushima M, Yamamoto K, Yasuda O, Oguro R, Yamamoto-Hanasaki H, Tatara Y, Takeya Y, Rakugi H. Klotho protein diminishes endothelial apoptosis and senescence

via a mitogen-activated kinase pathway. Geriatr Gerontol Int. 2011; 11:510–516. [PubMed: 21518171]

Makris N, Papadimitriou GM, van der Kouwe A, Kennedy DN, Hodge SM, Dale AM, Benner T, Wald LL, Wu O, Tuch DS, et al. Frontal connections and cognitive changes in normal aging rhesus monkeys: a DTI study. Neurobiology of aging. 2007; 28:1556–1567. [PubMed: 16962214]

Mason JL, Toews A, Hostettler JD, Morell P, Suzuki K, Goldman JE, Matsushima GK. Oligodendrocytes and progenitors become progressively depleted within chronically demyelinated lesions. The American journal of pathology. 2004; 164:1673–1682. [PubMed: 15111314]

Massa PT, Saha S, Wu C, Jarosinski KW. Expression and function of the protein tyrosine phosphatase SHP-1 in oligodendrocytes. Glia. 2000; 29:376–385. [PubMed: 10652447]

Meakin SO, MacDonald JI, Gryz EA, Kubu CJ, Verdi JM. The signaling adapter FRS-2 competes with Shc for binding to the nerve growth factor receptor TrkA. A model for discriminating proliferation and differentiation. The Journal of biological chemistry. 1999; 274:9861–9870. [PubMed: 10092678]

Medici D, Razzaque MS, Deluca S, Rector TL, Hou B, Kang K, Goetz R, Mohammadi M, Kuro OM, Olsen BR, et al. FGF-23-Klotho signaling stimulates proliferation and prevents vitamin D-induced apoptosis. J Cell Biol. 2008; 182:459–465. [PubMed: 18678710]

Mi S, Miller RH, Lee X, Scott ML, Shulag-Morskaya S, Shao Z, Chang J, Thill G, Levesque M, Zhang M, et al. LINGO-1 negatively regulates myelination by oligodendrocytes. Nature neuroscience. 2005; 8:745–751.

Nagai R, Saito Y, Ohyama Y, Aizawa H, Suga T, Nakamura T, Kurabayashi M, Kuroo M. Endothelial dysfunction in the klotho mouse and downregulation of klotho gene expression in various animal models of vascular and metabolic diseases. Cell Mol Life Sci. 2000; 57:738–746. [PubMed: 10892340]

Nagai T, Yamada K, Kim HC, Kim YS, Noda Y, Imura A, Nabeshima Y, Nabeshima T. Cognition impairment in the genetic model of aging klotho gene mutant mice: a role of oxidative stress. FASEB journal : official publication of the Federation of American Societies for Experimental Biology. 2003a; 17:50–52. [PubMed: 12475907]

Nagai T, Yamada K, Kim HC, Kim YS, Noda Y, Imura A, Nabeshima Y, Nabeshima T. Cognition impairment in the genetic model of aging klotho gene mutant mice: a role of oxidative stress. Faseb J. 2003b; 17:50–52. [PubMed: 12475907]

Ogawa Y, Schafer DP, Horresh I, Bar V, Hales K, Yang Y, Susuki K, Peles E, Stankewich MC, Rasband MN. Spectrins and ankyrinB constitute a specialized paranodal cytoskeleton. The Journal of neuroscience : the official journal of the Society for Neuroscience. 2006; 26:5230–5239. [PubMed: 16687515]

Oh SY, Chen CD, Abraham CR. Cell-type dependent modulation of Notch signaling by the amyloid precursor protein. Journal of neurochemistry. 2010; 113:262–274. [PubMed: 20089128]

Ong SH, Guy GR, Hadari YR, Laks S, Gotoh N, Schlessinger J, Lax I. FRS2 proteins recruit intracellular signaling pathways by binding to diverse targets on fibroblast growth factor and nerve growth factor receptors. Molecular and cellular biology. 2000; 20:979–989. [PubMed: 10629055]

Peters A. The effects of normal aging on myelinated nerve fibers in monkey central nervous system. Frontiers in neuroanatomy. 2009; 3:11. [PubMed: 19636385]

Rakugi H, Matsukawa N, Ishikawa K, Yang J, Imai M, Ikushima M, Maekawa Y, Kida I, Miyazaki J, Ogihara T. Anti-oxidative effect of Klotho on endothelial cells through cAMP activation. Endocrine. 2007; 31:82–87. [PubMed: 17709902]

Rasband MN, Kagawa T, Park EW, Ikenaka K, Trimmer JS. Dysregulation of axonal sodium channel isoforms after adult-onset chronic demyelination. Journal of neuroscience research. 2003; 73:465–470. [PubMed: 12898531]

Repa JJ, Mangelsdorf DJ. The role of orphan nuclear receptors in the regulation of cholesterol homeostasis. Annual review of cell and developmental biology. 2000; 16:459–481.

Rosene DL, Roy NJ, Davis BJ. A cryoprotection method that facilitates cutting frozen sections of whole monkey brains for histological and histochemical processing without freezing artifact. J Histochem Cytochem. 1986; 34:1301–1315. [PubMed: 3745909]

Shih PH, Yen GC. Differential expressions of antioxidant status in aging rats: the role of transcriptional factor Nrf2 and MAPK signaling pathway. Biogerontology. 2007; 8:71–80. [PubMed: 16850181]

Shimada T, Takeshita Y, Murohara T, Sasaki K, Egami K, Shintani S, Katsuda Y, Ikeda H, Nabeshima Y, Imaizumi T. Angiogenesis and vasculogenesis are impaired in the precocious-aging klotho mouse. Circulation. 2004; 110:1148–1155. [PubMed: 15302783]

Shiozaki M, Yoshimura K, Shibata M, Koike M, Matsuura N, Uchiyama Y, Gotow T. Morphological and biochemical signs of age-related neurodegenerative changes in klotho mutant mice. Neuroscience. 2008; 152:924–941. [PubMed: 18343589]

Sloane J, Hinman J, Lubonia M, Hollander W, Abraham C. Age-dependent myelin degeneration and proteolysis of oligodendrocyte proteins is associated with the activation of calpain-1 in the rhesus monkey. J Neurochem. 2003; 84:157–168. [PubMed: 12485412]

Sloane J, Vartanian T. Myosin Va controls oligodendrocyte morphogenesis and myelination. J Neurosci. 2007; 27:11366–11375. [PubMed: 17942731]

Subramanian A, Tamayo P, Mootha V, Mukherjee S, Ebert B, Gillette M, Paulovich A, Pomeroy S, Golub T, Lander E, et al. Gene set enrichment analysis: a knowledge-based approach for interpreting genome-wide expression profiles. Proc Natl Acad Sci U S A. 2005; 102:15545–15550. [PubMed: 16199517]

Taveggia C, Feltri ML, Wrabetz L. Signals to promote myelin formation and repair. Nature reviews Neurology. 2010; 6:276–287.

Thurston RD, Larmonier CB, Majewski PM, Ramalingam R, Midura-Kiela M, Laubitz D, Vandewalle A, Besselsen DG, Muhlbauer M, Jobin C, et al. Tumor necrosis factor and interferon-gamma down-regulate Klotho in mice with colitis. Gastroenterology. 2010; 138:1384–1394. 1394, e1381–1382. [PubMed: 20004202]

Trapp, BD.; Kidd, GJ. Structure of the myelinated axon. In: Lazzarini, RA., editor. Myelin biology and disorders. Elsevier Academic Press; London: 2004. p. 3-22.

Urakawa I, Yamazaki Y, Shimada T, Iijima K, Hasegawa H, Okawa K, Fujita T, Fukumoto S, Yamashita T. Klotho converts canonical FGF receptor into a specific receptor for FGF23. Nature. 2006; 444:770–774. [PubMed: 17086194]

Vabnick I, Novakovic SD, Levinson SR, Schachner M, Shrager P. The clustering of axonal sodium channels during development of the peripheral nervous system. The Journal of neuroscience : the official journal of the Society for Neuroscience. 1996; 16:4914–4922. [PubMed: 8756423]

Van't Veer A, Du Y, Fischer TZ, Boetig DR, Wood MR, Dreyfus CF. Brain-derived neurotrophic factor effects on oligodendrocyte progenitors of the basal forebrain are mediated through trkB and the MAP kinase pathway. Journal of neuroscience research. 2009; 87:69–78. [PubMed: 18752299]

Wang L, Schuster GU, Hultenby K, Zhang Q, Andersson S, Gustafsson JA. Liver X receptors in the central nervous system: from lipid homeostasis to neuronal degeneration. Proceedings of the National Academy of Sciences of the United States of America. 2002; 99:13878–13883. [PubMed: 12368482]

Waxman SG. Demyelinating diseases--new pathological insights, new therapeutic targets. The New England journal of medicine. 1998; 338:323–325. [PubMed: 9445415]

Wegner M. Transcriptional control in myelinating glia: the basic recipe. Glia. 2000; 29:118–123. [PubMed: 10625329]

Whitney KD, Watson MA, Collins JL, Benson WG, Stone TM, Numerick MJ, Tippin TK, Wilson JG, Winegar DA, Kliewer SA. Regulation of cholesterol homeostasis by the liver X receptors in the central nervous system. Molecular endocrinology. 2002; 16:1378–1385. [PubMed: 12040022]

Wisco JJ, Killiany RJ, Guttmann CR, Warfield SK, Moss MB, Rosene DL. An MRI study of age-related white and gray matter volume changes in the rhesus monkey. Neurobiology of aging. 2008; 29:1563–1575. [PubMed: 17459528]

Wolf I, Levanon-Cohen S, Bose S, Ligumsky H, Sredni B, Kanety H, Kuro-o M, Karlan B, Kaufman B, Koeffler HP, et al. Klotho: a tumor suppressor and a modulator of the IGF-1 and FGF pathways in human breast cancer. Oncogene. 2008; 27:7094–7105. [PubMed: 18762812]

Yamamoto M, Clark JD, Pastor JV, Gurnani P, Nandi A, Kurosu H, Miyoshi M, Ogawa Y, Castrillon DH, Rosenblatt KP, et al. Regulation of oxidative stress by the anti-aging hormone klotho. J Biol Chem. 2005; 280:38029–38034. [PubMed: 16186101]

Younes-Rapozo V, Felgueiras LO, Viana NL, Fierro IM, Barja-Fidalgo C, Manhaes AC, Barradas PC. A role for the MAPK/ERK pathway in oligodendroglial differentiation in vitro: stage specific effects on cell branching. International journal of developmental neuroscience : the official journal of the International Society for Developmental Neuroscience. 2009; 27:757–768. [PubMed: 19729058]

Zeldich E, Koren R, Nemcovsky C, Weinreb M. Enamel matrix derivative stimulates human gingival fibroblast proliferation via ERK. J Dent Res. 2007; 86:41–46. [PubMed: 17189461]

Zhao Y, Banerjee S, Dey N, LeJeune WS, Sarkar PS, Brobey R, Rosenblatt KP, Tilton RG, Choudhary S. Klotho depletion contributes to increased inflammation in kidney of the db/db mouse model of diabetes via RelA (serine)536 phosphorylation. Diabetes. 2011; 60:1907–1916. [PubMed: 21593200]

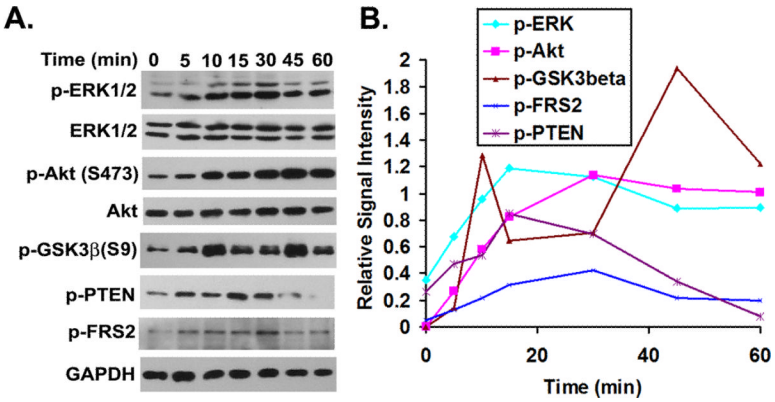

Figure 1.

Phosphorylation kinetic analysis of Klotho treated OPCs. A. OPCs were treated with Klotho for the times indicated and the cell lysates were analyzed by Western blotting for protein phosphorylation of the proteins indicated. B. Kinetics of the signal intensity based on band densitometry as in A. Results represent the average of two independent experiments. Phosphorylated ERK1/2 and Akt are normalized to total ERK1/2 and Akt, respectively. All other phosphorylated proteins are normalized to GAPDH internal control.

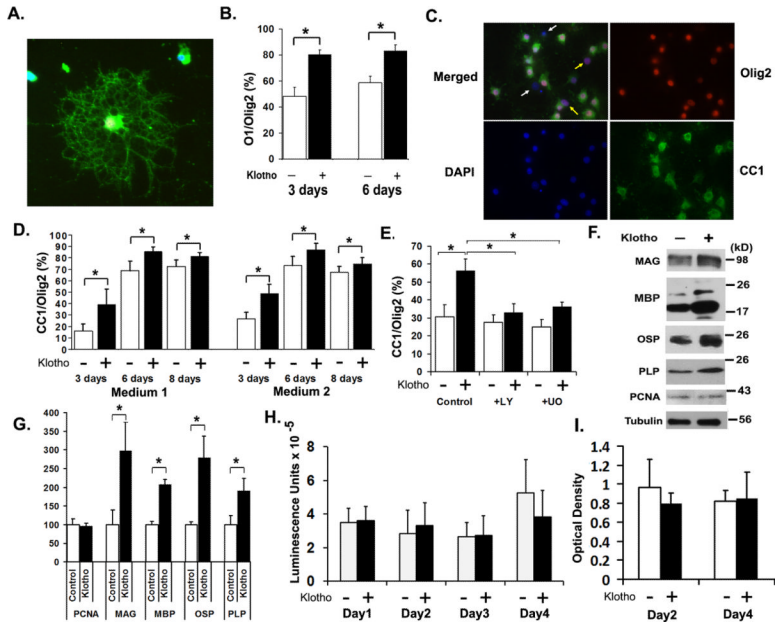

Figure 2.

Klotho effects *in vitro* on primary OPCs. A–D. Klotho enhances oligodendrocyte maturation. Rat OPCs were treated with Klotho (+ Klotho) or with PBS (Control) for 3 days, and then immunostained for the mature oligodendrocyte marker O1 (green), and pan-oligodendrocyte marker Olig2 (red). A. A typical O1 staining of a differentiated oligodendrocyte. B. Statistical analysis of O1 and Olig2 staining of OPCs at 3 and 6 days treatment with Klotho or PBS. Asterisks (*) indicate statistical significance of $p<0.005$ by *t*-test. Error bars indicate standard deviation. C. Immunostaining of OPCs with antibodies to the mature oligodendrocyte marker CC-1 (green), and pan-oligodendrocyte marker Olig2 (red). Cell nuclei were stained with DAPI (blue). White arrows in the merged image indicate non-oligodendrocytic cells, and yellow arrows indicate undifferentiated oligodendrocytes. D. Statistical analysis of the ratio of CC-1 to Olig2 staining of OPCs at 3, 6 and 8 days treatment with Klotho or PBS in medium 1 (OPC culture medium containing CNTF and T3) or medium 2 (OPC culture medium containing CNTF, T3 and NT3). Asterisks (*) indicate statistical significance of $p<0.005$ by *t*-test. Error bars indicate standard deviation. E. Klotho enhances OPC maturation via ERK and Akt signaling. Rat OPCs were treated with 0.5 μM LY294002 (LY) (for Akt inhibition) or 1 μM UO126 (UO) (for ERK inhibition) for 30 min before Klotho (KL) was added. OPCs were treated for 3 days, and then immunostained as in D. Statistical analysis of the results is plotted. F. Klotho enhances major myelin proteins expression in rat OPCs. OPCs were treated with or without Klotho for 6 days in culture medium containing CNTF and T3, and blotted with the antibodies indicated with tubulin as loading control. G. The relative signal intensity based on band densitometry was plotted as relative percentage to control without Klotho treatment. Results represent the average of three to five independent experiments. All proteins are normalized to tubulin internal control. Asterisks (*) indicate statistical significance of $p<0.005$ by *t*-test. Error bars indicate standard deviation. H. Klotho does not affect OPC cell viability. CellTiterGlo assay was used to assess Klotho's effect on OPC cell viability after 1–4 days of Klotho treatment. Error bars indicate standard deviation. Results represent the average of six independent experiments. I. Klotho does not affect OPC cell proliferation. Cell numbers were assayed by crystal violet staining at day 2 and day 4 after Klotho treatment. Error bars indicate standard deviation. Results represent the average of three independent experiments.

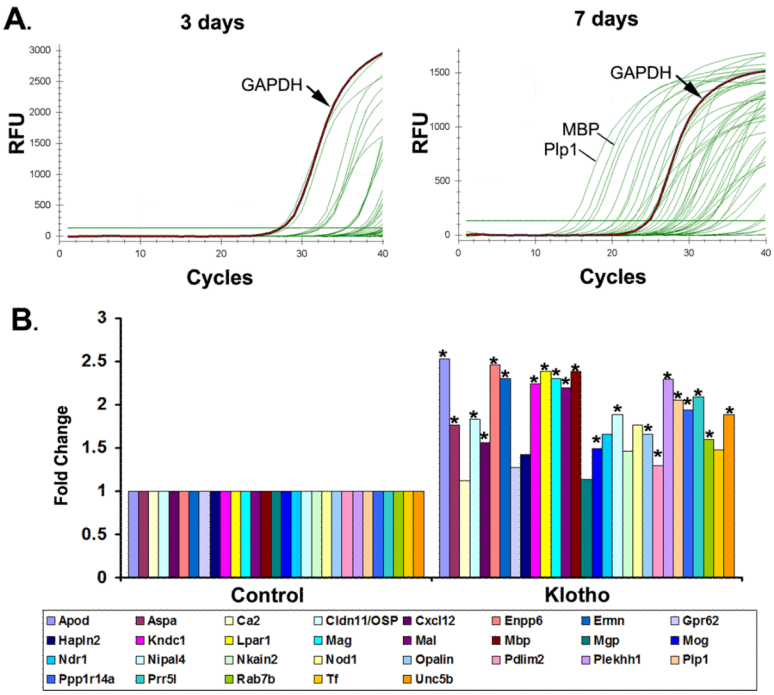

Figure 3.

Quantitative real-time RT-PCR confirmation of the effect of Klotho on OPC maturation. A. Representative qPCR results of differentiated OPCs for 3 days and 7 days. The housekeeping gene GAPDH and the top two expressed genes, MBP and Plp1 are indicated. B. Fold change results of the up-regulated genes by qPCR analysis of RNA from OPCs treated with Klotho for 7 days compared to control. OPCs were cultured in medium containing bFGF and PDGF for 3 days, and then changed to the differentiation medium with CNTF and T3 with or without Klotho for 7 days. Asterisks (*) indicate statistical significance of $p<0.05$ by *t*-test.

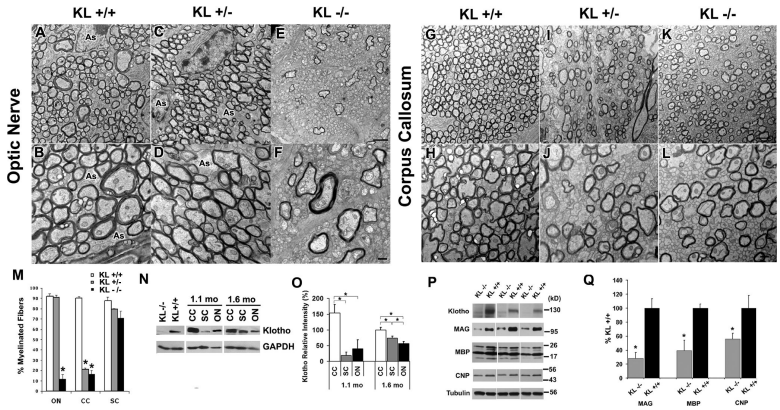

Figure 4.

Klotho knockout mice exhibit impaired myelination. A–L, 4 ½ week old Klotho +/+, +/− or −/− mice were processed for electron microscopy. Cross-sectional images show examples of myelination patterns for optic nerve (A–F) at 2900× (A, C and E) and 5800× (B, D and F) and corpus callosum (G–L) at 2900× (G, I and K) and 5800× (H, J and L). Scale bars represent 2 microns in E and 500 nm in F. As: astrocyte. M, The number of myelinated and unmyelinated axons were counted and graphed as percentage of myelinated fibers. Averages represent axonal counts analyzed from 3–6 different images. The asterisks (*) indicate significance at $p < 0.0001$ by *t*-test. Error bars indicate standard deviation. ON: optic nerve, CC: corpus callosum, SC: spinal cord. N, Klotho expression in CC, SC and ON. Western blot analysis of Klotho from the lysates of 1.1 and 1.6 months old control mice CC, SC and ON tissues. O. Statistical analysis of Klotho expression in N with tubulin as loading control. Asterisks (*) indicate statistical significance of $p<0.05$ by *t*-test. Error bars indicate standard deviation. Sample size is n=4 for each age. P. Major myelin proteins were largely reduced in Klotho knockout mice. Western blot analysis of myelin markers from the brain lysates of 8 weeks old Klotho knockout (KL −/−) and control (KL +/+) mice. Q. Statistical analysis of the myelin markers in P with tubulin as control. Asterisks (*) indicate statistical significance of $p<0.05$ by *t*-test. Error bars indicate standard deviation.

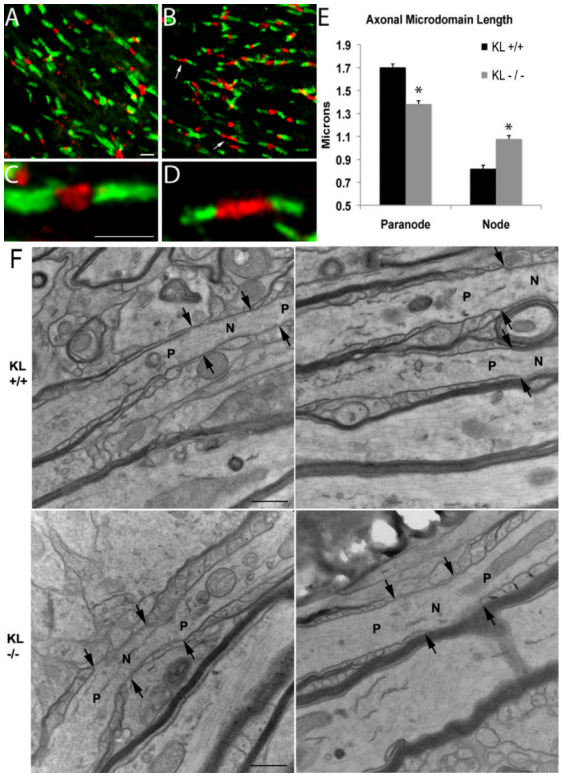

Figure 5.

Axonal microdomains are altered in Klotho −/− mice. Five sections each of corpus callosum from two wild-type and two homozygous Klotho −/− mice were stained for caspr (green) and beta-IV spectrin (red). Wild-type mice have normal compact paranodal and nodal structure (A and C), while Klotho −/− mice show an abundance of shorter paranodal segments and longer nodal segments (arrows, B and D). Measurements of nodal and paranodal length show a statistically significant decrease in paranodal length in Klotho −/− mice associated with a significant increase in nodal length (E). Asterisks (*) indicate statistical significance of $p<0.001$ by *t*-test. Scale bar = 2 microns. F. Electron microscopic longitudinal section analysis of nodes of Ranvier in corpus callosum from wild-type (KL +/+) and Klotho −/− (KL −/−) mice at 13,000×. Arrows indicate the junction between node and paranode. N: node; P: paranode. Scale bars represent 500 nm.

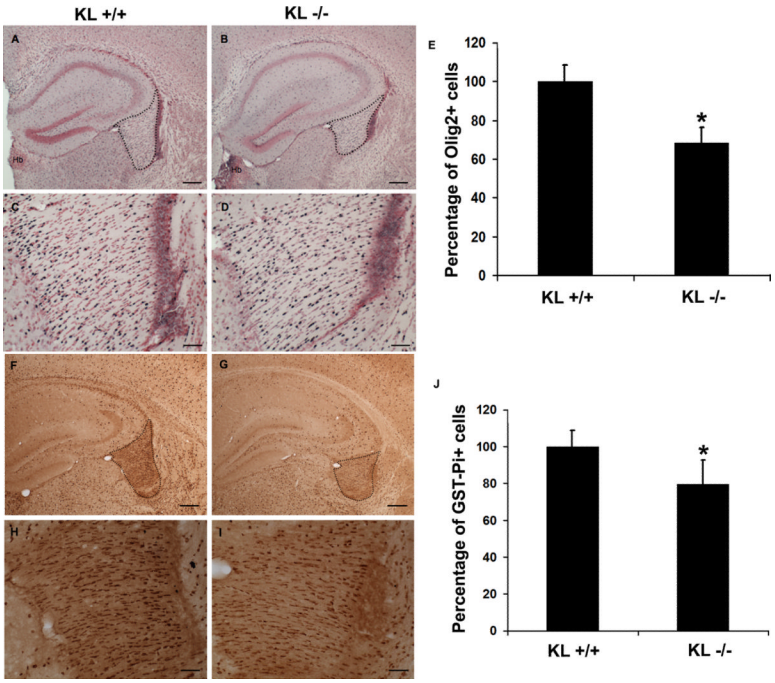

Figure 6.

Immunohistochemistry and quantitative analysis of expression of Olig2 and GST-Pi in brain sections from 5 week old Klotho +/+ and −/− mice. A–D, IHC images show examples of Olig2 nuclear staining patterns at 4× (A and B) and 20× (C and D). Scale bars represent 200 microns in A and B, and 50 microns in C and D. A and C: KL +/+, B and D: KL −/−. The fimbria region is outlined. Hb: Habenula. E, Cell counting of Olig2-positive was performed as described in methods. The number of Olig2 + cells in fimbria were counted and the percentage of Olig2 + cells in KL +/+ and KL −/− graphed. The asterisk (*) indicates significance at $p < 0.01$ by *t*-test. Error bars indicate standard deviation. F–I, IHC of brain sections with antibodies to the mature oligodendrocyte marker GST-Pi at 4× (F and G) and 20× (H and I). Scale bars represent 200 microns in F and G, and 50 microns in H and I. J, Quantitation of GST-Pi-positive cells as described in methods. The GST-Pi + cells in fimbria were counted and the percentage of GSTPi+ cells in KL +/+ and KL −/− graphed. The asterisk (*) indicates significance at $p < 0.05$ by *t*-test. Error bars indicate standard deviation.

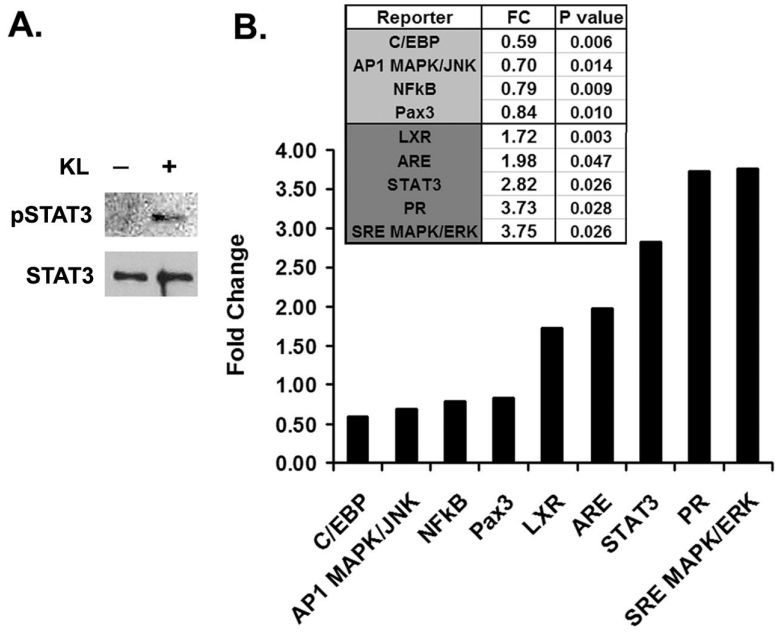

Figure 7.

Transcription factors involved in Klotho regulation of OPCs. A Western blot analysis of STAT3 phosphorylation upon Klotho treatment of OPC cells. B. Luciferase assay of luciferase reporters in OPC cells. OPCs were transfected with the reporter plasmids with Renilla luciferase and treated with or without Klotho for 24 hrs followed by luciferase assay. The fold change comparing Klotho treated to control is shown. P values indicate statistical significance by *t*-test.

Table 1

List of myelin related genes used in qPCR analysis comparing gene expression of Klotho −/− and +/+ mice brain samples at 8 weeks of age. Fold change represents Klotho −/− compared to Klotho +/+ as control. N=4 for each group.

Symbol	Description	Fold Change	p value
Aspa	aspartoacylase	−1.99	**0.0374**
CNP	2',3'-cyclic nucleotide 3' phosphodiesterase	**−2.26**	**0.0419**
EDG2	lysophosphatidic acid receptor 1	**−2.18**	**0.0271**
Enpp2	ectonucleotide pyrophosphatase/phosphodiesterase 2	−1.73	**0.0345**
Erbb3	v-erb-b2 erythroblastic leukemia viral oncogene homolog 3	−1.92	**0.0196**
Klk6	kallikrein related-peptidase 6	**−7.35**	**0.0237**
MAG	myelin-associated glycoprotein	**−3.97**	**0.0266**
MBP	myelin basic protein	**−4.68**	**0.0189**
MAL	myelin and lymphocyte protein, T-cell differentiation protein	**−2.09**	**0.0479**
MOBP	myelin-associated oligodendrocytic basic protein	**−3.15**	**0.0132**
MOG	myelin oligodendrocyte glycoprotein	**−2.88**	**0.0045**
Olig2	oligodendrocyte transcription factor 2	−1.54	0.1581
Pllp	plasma membrane proteolipid	**−2.26**	**0.0051**
Plp1	proteolipid protein (myelin) 1	**−2.30**	**0.0097**
Pmp22	peripheral myelin protein 22	**−3.94**	0.0715

P values of less than 0.05 and Fold change greater than −2 are in bold.

Table 2

Signal Transduction 45-pathway Reporter Array.

Reporter	Pathway	Transciption Factor
AARE Reporter	Amino Acid Deprivation Response	ATF4/ATF3/ATF2
AR Reporter	Androgen Receptor	Androgen Receptor
ARE Reporter	Antioxidant Response	Nrf2 & Nrf1
ATF6 Reporter	ATF6	ATF6
C/EBP Reporter	C/EBP	C/EBP
CRE Reporter	cAMP/PKA	CREB
E2F Reporter	Cell Cycle	E2F/DP1
p53 Reporter	p53/DNA Damage	p53
EGR1 Reporter	EGR1	EGR1
ERSE Reporter	Endoplasmic Reticulum Stress	CBF/NF-Y/YY1
ERE Reporter	Estrogen Receptor	Estrogen Receptor
GATA Reporter	GATA	GATA
GRE Reporter	Glucocorticoid Receptor	Glucocorticoid Receptor
HSR Reporter	Heat Shock Response	HSF
MTF1 Reporter	Heavy Metal Stress	MTF1
GLI Reporter	Hedgehog	GLI
HNF4 Reporter	Hepatocyte Nuclear Factor 4	HNF4
HIF Reporter	Hypoxia	HIF-1
IRF1 Reporter	Interferon Regulation	IRF1
ISRE Reporter	Type I Interferon	STAT1/STAT2
GAS Reporter	Interferon Gamma	STAT1/STAT1
KLF4 Reporter	KLF4	KLF4
LXR Reporter	Liver × Receptor	LXRa
SRE Reporter	MAPK/ERK	Elk-1/SRF
AP1 Reporter	MAPK/JNK	AP-1
MEF2 Reporter	MEF2	MEF2
Myc Reporter	c-myc	Myc/Max
Nanog Reporter	Nanog	Nanog
RBP-Jk Reporter	Notch	RBP-Jk
NFκB Reporter	NFκB	NFκB
Oct4 Reporter	Oct4	Oct4
Pax6 Reporter	Pax6	Pax6
FOXO Reporter	PI3K/AKT	FOXO
NFAT Reporter	PKC/Ca++	NFAT
PPAR Reporter	PPAR	PPAR
PR Reporter	Progesterone Receptor	Progesterone Receptor
RARE Reporter	Retinoic Acid Receptor	Retinoic Acid Receptor

Reporter	Pathway	Transciption Factor
RXR Reporter	Retinoid × Receptor	Retinoid × Receptor
Sox2 Reporter	Sox2	Sox2
SP1 Reporter	SP1	SP1
STAT3 Reporter	STAT3	STAT3
SMAD Reporter	TGFβ	SMAD2/SMAD3/SMAD4
VDR Reporter	Vitamin D Receptor	Vitamin D Receptor
TCF/LEF Reporter	Wnt	TCF/LEF
XRE Reporter	Xenobiotic	AhR

Table 3

Transcriptional regulatory element sequence information of the luciferase reporters involved in Klotho-dependent responses in OPCs.

Reporter	Pathway	Transcriptional Regulatory Element Sequence
AP1	MAPK/JNK	TGAGTCAG
ARE	Antioxidant Response	AACATTGCATCATCCCCGC
C/EBP	C/EBP	ATTGCGCAAT
LXR	Liver × Receptor	TGAATGACCAGCAGTAACCTCAGC
NFkB	NFkB	GGGACTTTCC
PR	Progesterone Receptor	GGGACATGGTGTTCT
SRE	MAPK/ERK	GGATGTCCATATTAGGA
STAT3	STAT3	GTCGACATTTCCCGTAAATCGTCGA

Table 4

Primers information of the top 45 corresponding rat oligodendrocyte maturation enriched genes.

Symbol	Accession	Size	Forward	Reverse
Nod1	NM_001109236	182	GCTCGTCACAGACTCTGGTT	AAGGGTGGGAACTGATTCTC
Ermn	NM_001008311	182	TCTTCCACTGCCTTATTTGC	TGGGACAATGCTTACCTGAT
Nipal	NM_001106995	198	TCTCCGTTGACAACTTAGCC	GGTCCATGTGTCAAGCCTAC
Opalin	NM_001017386	152	CCGCTCTTCGGTATTTGTTA	AAGGACAAATGGTGTCCAGA
Tmem125	NM_001107967	198	CCGTCAGAGATAAAGCCTCA	GAAGGGTTAGGGGTCAGGTA
Prr5l	NM_001080150	231	GTGGAGGAGAAGATCAAGCA	AGAAGGCAACTTGGACTGTG
Ndrl	NM_001011991	151	GGAAAGTTGGGCACCTTATT	CAGAAAAACAGGTTGCGAGT
Tppp3	NM_001009639	162	AGGAGAGTTTCCGCAAGTTT	TTGCCTTGACTTTGGAGAAG
Rab7b	NM_001109328	151	GCAGGACTGGAAGAACTGAA	AGAGAGGTCTTTCCCACACC
Mog	NM_022668	157	GCGCTTCAACATTACGATCT	ACCCTGGCTCATTTAGCTTT
Ppp1r14a	NM_130403	111	ATGCCAGATGAGGTCAACAT	GAAGTCCTCTGTGGGATTCA
Ndrg1	NM_001011991	151	GGAAAGTTGGGCACCTTATT	CAGAAAAACAGGTTGCGAGT
Mobp	NM_012720	104	ATCACCCCAGAGATTCTTCC	GCATTGGAGCGAGAATTAAA
Cldn11	NM_053457	191	CACCTCTTGGTTGCCTTAAA	TATTTCTCTCCCAACCCACA
Itih3	NM_017351	160	GGAAGCTGGAGAAGTTCACA	GCGTCGATCTCAAAGTGTCT
Ttyh2	XM_221081	114	ACCATGCAGATCCAAGTTGT	CAGGCTGGTCTCAGAGTTGT
Kndc1	XM_002728817	162	CCTGCAGGACCTTCTGTCTA	CCAAAGAACACAGTCCCATC
St18	NM_153310	213	TTTATCCCTTGCGAGAACAG	TTCAGCCTGTAGGGCAATAG
Lpar1	NM_053936	213	ATGTTCAACACGGGACCTAA	AATGGCCATAGTCCAGATGA
Enpp6	NM_001107311	194	TCTCCATCCTCAGTCTTTGC	GGGCATCCTCACTGATGTAG
Aspa	NM_024399	216	CGTGTACCCAGTGTTTGTGA	CAAGGTGCTGAGGAAAAGAA
Mag	NM_017190	154	AACCTGTCTGTGGAGTTTGC	CTGTCTCGTTCACAGTCACG
Gpr37	NM_010338	254	TCTACCCATTGACCCAAGAA	CTTGCAGGAGAAATCTTCCA
Pdlim2	NM_053326	246	AGATCCTTGGGGAAGTCATC	AGCACACAAAGCAAGTGTCA
Sgk2	NM_134463	299	CCTATGCCTAGCAGGAAACA	TTGTGGTCTCGTAACCCAAT
Mgp	NM_012862	298	CAGCCCTGTGCTATGAATCT	CTCCGTAACAAAGCGACTGT
Apod	NM_012777	190	CAGGTCTCTTCACCACAACC	TTGATGTTTCCGTTCTCCAT
S1pr5	NM_021775	166	CATGGACAACAACAAAACGA	CAACAAGACTTCCCACAACC
Nkain2	XM_002728643	179	TGGATATCAGTGGGCACCTA	AGAGATCTCCAGCCTCCAAA
Adamts4	NM_023959	114	CCATGCCATGTGTCAGACTA	TTGAAGTCCTTGAGCTGGTC
fhd1	NM_001109310	168	GAACTTCTTCGAAGCCAAGG	TCAGGTCAGCAGGACTATGC
Adssl1	XM_001072867	242	GGGAATCGGACCAACTTACT	GACCATGGAGTGCCTCATAC
Plekhh1	NM_001108036	126	GCCTAATCCAGCTCCTTTTC	ATGTTGGTTCCCAGACTTGA
Gpr62	XM_576464	101	TCTGGGCAGAAGACTACCTG	CTGGAGGGGTCCTCAGTTAT
Plp1	NM_030990	206	TGATGCCAGAATGTATGGTG	TGAGTTTAAGGACGGCAAAG
Gjc2	NM_001100784	244	GAACTGTGTCCCAGGAATTG	CTAAAGGCCTCCTTCAGGTC
Unc5b	NM_022207	170	CGAATACGAGAGGTGCAGAT	AGAGGCTCCTGGTCAAAGTT

Symbol	Accession	Size	Forward	Reverse
Ca2	NM_019291	129	TGTCAGCAGTGAGCAGATGT	AAGGACGCCTTGATCTTTCT
Hapln2	NM_022285	124	CCATCTTGAGAGCCTCTTCC	GCACGCCTTAGTACTGCAAG
Tf	NM_001013110	178	CAAGCCTCTTGAGAAAGCTG	CACATCTCCACCTCCATCTC
Mal	NM_012798	203	ACCTTCCCTGACTTGCTCTT	TCCAGTGTGATCCAGGAAGT
Il23a	NM_130410	237	GCTTTGGCCAGAATCTGTAA	CAAAATTTCCCTTCCCACTT
Mbp	NM_001025291	236	TGGCCACTTCTCACTTTAGG	AGGTGTCCGTGGACATTAGA
Bace2	NM_001002802	185	CCAAAAGGCTTCAACAGCTC	ATGTCCGGAATTTTTGCTTG
Cxcl12	NM_022177	243	GAGGCTCCTTTTTCCAGTTC	CCAAGTGAGAGGAAAGCAAA